



CHORUS

This is the accepted manuscript made available via CHORUS. The article has been published as:

Spin-lattice coupling mediated multiferroicity in $(\text{ND}_{4})_{2}\text{FeCl}_{5}\cdot\text{D}_{2}\text{O}$

W. Tian, Huibo Cao, Jincheng Wang, Feng Ye, M. Matsuda, J.-Q. Yan, Yaohua Liu, V. O. Garlea, Harish K. Agrawal, B. C. Chakoumakos, B. C. Sales, Randy S. Fishman, and J. A. Fernandez-Baca

Phys. Rev. B **94**, 214405 — Published 7 December 2016

DOI: [10.1103/PhysRevB.94.214405](https://doi.org/10.1103/PhysRevB.94.214405)

Spin-lattice coupling mediated multiferroicity in $(\text{ND}_4)_2\text{FeCl}_5\cdot\text{D}_2\text{O}$

W. Tian,^{1,*} Huibo Cao,¹ Jincheng Wang,¹ Feng Ye,¹ M. Matsuda,¹
J.-Q. Yan,^{2,3} Yaohua Liu,¹ V. O. Garlea,¹ Harish K. Agrawal,⁴ B. C.
Chakoumakos,¹ B. C. Sales,² Randy S. Fishman,² and J. A. Fernandez-Baca^{1,5}

¹*Quantum Condensed Matter Division,*

Oak Ridge National Laboratory, Oak Ridge, Tennessee 37831, USA

²*Materials Science and Technology Division,*

Oak Ridge National Laboratory, Oak Ridge, Tennessee 37831, USA

³*Department of Materials Science and Engineering,*

University of Tennessee, Knoxville, Tennessee 37996, USA

⁴*Instrument and Source Division, Oak Ridge National Laboratory,*

Oak Ridge, Tennessee 37831, USA

⁵*Department of Physics and Astronomy,*

The University of Tennessee, Knoxville, Tennessee 37996, USA

(Dated: November 15, 2016)

Abstract

We report a neutron diffraction study of the multiferroic mechanism in $(\text{ND}_4)_2\text{FeCl}_5\cdot\text{D}_2\text{O}$, a molecular compound that exhibits magnetically induced ferroelectricity. This material exhibits two successive magnetic transitions on cooling: a long-range order transition to an incommensurate (IC) collinear sinusoidal spin state at $T_N=7.3$ K, followed by a second transition to an IC cycloidal spin state at $T_{FE}=6.8$ K, the later of which is accompanied by spontaneous ferroelectric polarization. The cycloid structure is strongly distorted by spin-lattice coupling as evidenced by the observations of both odd and even higher-order harmonics associated with the cycloid wave vector, and a weak commensurate phase that coexists with the IC phase. The 2nd-order harmonic appears at T_{FE} , thereby providing unambiguous evidence that the onset of the electric polarization is accompanied by a lattice modulation due to spin-lattice interaction. The neutron results, in conjunction with the negative thermal expansion and large magnetostriction observed in Ref. 19, indicate that spin-lattice coupling plays a critical role in the FE mechanism of $(\text{ND}_4)_2\text{FeCl}_5\cdot\text{D}_2\text{O}$.

PACS numbers: 77.80.-e, 75.25.-j, 61.50.Ks, 75.30.Kz

“Improper multiferroics” (also referred as type-II magnetic multiferroics) are a unique group of materials that exhibit direct coupling between magnetism and electric polarization [1, 2]. In these magnetically induced multiferroics, the magnetoelectric (ME) effect is strong and the onset of ferroelectricity arises directly from magnetic order that breaks spatial inversion symmetry. Due to the strong ME effect, there has been enormous interest in these materials motivated by their potential applications in novel multifunctional devices. However, natural single-phase magnetically driven multiferroics are rare, most currently known materials that exhibit such effect are transition-metal oxides such as TbMnO_3 [3–9], MnWO_4 [10], $\text{Ni}_3\text{V}_2\text{O}_8$ [11], CuO [12], LiCuVO_4 [13], and CaCoMnO_3 [14]. It is thus of great interest to discover and investigate new multiferroics. Recently, the search has been extended to include molecular compounds and metal-organic framework materials (MOFs)[15] and several such materials have been discovered to be new multiferroics [16–18]. As one of the new directions for multiferroic research, molecular and MOFs multiferroics have been attracting considerable attention. Due to the relatively “soft” lattice compared to oxides, the emergent properties of such a system are usually experimentally accessible and are more sensitive to external perturbations, i.e. new phases can be induced by modest applied field and pressure. This offers a unique opportunity to test theoretical models that will shed light on the underlying multiferroic mechanism. In this paper, we report a neutron diffraction study of $(\text{NH}_4)_2\text{FeCl}_5\cdot\text{H}_2\text{O}$, a molecular compound that was recently discovered to exhibit magnetically induced multiferroicity [19]. Using both polarized and unpolarized neutrons, we show that the onset of the electric polarization is accompanied by a lattice modulation indicating spin-lattice coupling plays a critical role in the ferroelectric mechanism of $(\text{NH}_4)_2\text{FeCl}_5\cdot\text{H}_2\text{O}$.

$(\text{NH}_4)_2\text{FeCl}_5\cdot\text{H}_2\text{O}$ belongs to the erythrosiderite-type compounds $A_2[\text{FeX}_5\cdot\text{H}_2\text{O}]$, where A is an alkali metal or ammonium, and X is a halide ion [20–23]. It crystallizes in an orthorhombic structure at room temperature (space group $Pnma$) with a crystal structure consisting of distorted $[\text{FeCl}_5\cdot\text{H}_2\text{O}]^{2-}$ octahedra linked by a network of hydrogen bonds [19] as illustrated in Fig. 1 (a). The magnetic interactions in these materials are mediated via multiple superexchange pathways, such as $\text{Fe-Cl}\cdots\text{Cl-Fe}$, $\text{Fe-O}\cdots\text{Cl-Fe}$, and $\text{Fe-O-H}\cdots\text{Cl-Fe}$ involving hydrogen bonds, suggesting the presence of magnetic frustration in the system [23]. $(\text{NH}_4)_2\text{FeCl}_5\cdot\text{H}_2\text{O}$ [19] is the only compound that exhibits spontaneous electric polarization in the $A_2[\text{FeX}_5\cdot\text{H}_2\text{O}]$ series. In sharp contrast to other isostructural counterparts,

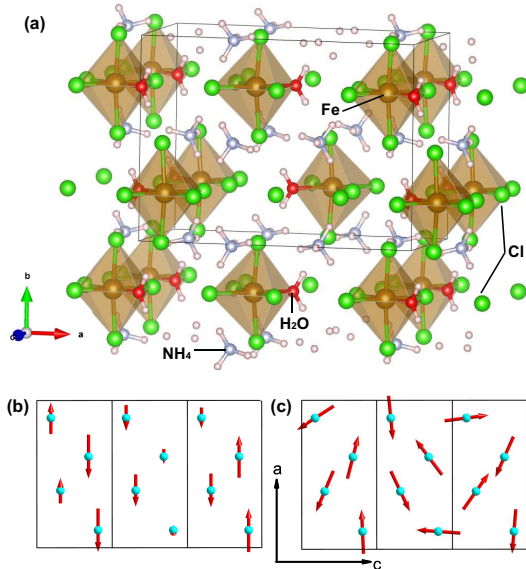


FIG. 1. (Color online) (a) Crystal structure of $(\text{NH}_4)_2\text{FeCl}_5 \cdot \text{H}_2\text{O}$. (b) IC collinear sinusoidal spin structure at 7 K in the paraelectric phase; (c) IC cycloidal-spiral spin structure at 4 K in the ferroelectric phase, as viewed along the b -axis (three unit cells along c -axis are plotted). Only magnetic Fe ions are shown in (b) and (c) for the purpose of clarity.

such as $(\text{K}, \text{Rb})_2\text{FeCl}_5 \cdot \text{H}_2\text{O}$ which undergo a single magnetic transition adopting a collinear antiferromagnetic (AFM) spin structure with moments along the a -axis [22] and have no spontaneous electric polarization, $(\text{NH}_4)_2\text{FeCl}_5 \cdot \text{H}_2\text{O}$ undergoes three transitions, a disorder-order transition associated with the motion of the NH_4 group at $T_s \sim 79$ K [24], and two magnetic transitions at $T_N \sim 7.3$ K and $T_{FE} \sim 6.8$ K, respectively. The material remains paraelectric below 79 K and spontaneous electric polarization only appears below T_{FE} . Consequently, it is crucial to know the magnetic structure and microscopic interactions to unveil the underlying mechanism responsible for the multiferroic properties in this compound. However, although the unusual low temperature magnetic transitions were first reported in 1970's [21], the determination of the full magnetic structure has been hampered due to the large amount of hydrogen atoms (40 H atoms per unit cell) in this compound.

To uncover the nature of the coupling between magnetism and ferroelectricity in this molecular compound, we performed neutron diffraction experiments on deuterated $(\text{ND}_4)_2\text{FeCl}_5 \cdot \text{D}_2\text{O}$ single crystals using the HB1, HB1A triple-axis spectrometer (TAS), and HB3A Four-Circle Diffractometer located at the High Flux Isotope Reactor (HFIR), and the Elastic Diffuse Scattering Spectrometer (CORELLI) at the Spallation Neutron Source (SNS) at Oak Ridge National Laboratory (ORNL) [25]. Our data show that $(\text{ND}_4)_2\text{FeCl}_5 \cdot \text{D}_2\text{O}$ undergoes an

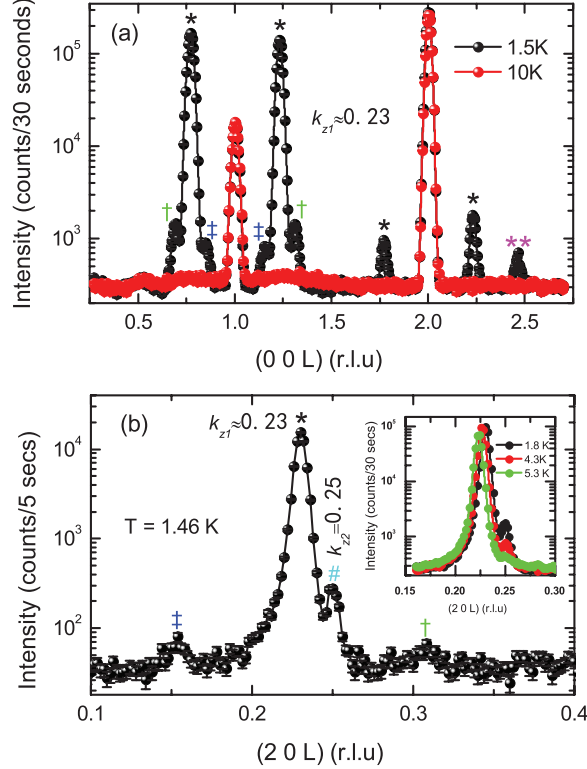


FIG. 2. (Color online) L-scans along both (0 0 L) and (2 0 L) with the intensity plotted on a logarithmic scale. (a) (0 0 L) scan measured at 1.5 K and 10 K. The primary IC satellites ($0\ 0\ n\pm k_{z1}$), and the 2nd ($0\ 0\ n\pm 2k_{z1}$), 3rd ($0\ 0\ n\pm 3k_{z1}$), 5th order ($0\ 0\ n\pm 5k_{z1}$) harmonic peaks are marked by *(black), **(pink), †(green) and ‡(blue), respectively (n is an integer). (b) (2 0 L) scan measured at 1.5 K reveals the coexistence of IC and commensurate phases. The primary IC satellites ($2\ 0\ n\pm k_{z1}$), 3rd ($2\ 0\ n\pm 3k_{z1}$), 5th-order ($2\ 0\ n\pm 5k_{z1}$) harmonic peaks and the commensurate peak ($2\ 0\ n\pm k_{z2}$) are marked by *(black), †(green), ‡(blue) and ‡ (cyan), respectively. Neutron data have been normalized to beam monitor count and the error bars are statistical in nature and represent one standard deviation.

incommensurate (IC) AFM long range order (LRO) transition at $T_N=7.3$ K. The primary magnetic satellite peak can be indexed with a propagation vector $k_1=(0\ 0\ k_{z1})$, $k_{z1} \approx 0.23$ at 1.5 K, consistent with the recent study by Rodríguez-Velamazán et al. [24]. To determine the magnetic structures associated with both the paraelectric phase between $T_{FE}<T<T_N$ and the ferroelectric phase below $T_{FE}=6.8$ K, sets of nuclear and magnetic reflections were collected at 7 K and 4 K at HB3A (wave length 1.546 Å). FullProf refinement of 4 K data confirms an IC cycloidal spiral spin structure with moments mainly confined in the ac -plane (moment size $\sim 4.08\ \mu_B$) consistent with Ref. 24. The magnetic structure at 7 K is found to be an IC collinear sinusoidal spin state along the a -axis, with a moment size of $\sim 2.17\ \mu_B$. The schematic magnetic structures at 7 K and 4 K are illustrated in Fig. 1 (b)

and (c), respectively. This indicates a magnetic structure change from collinear sinusoidal to cycloidal spiral at $T_{FE}=6.8$ K that suggests an inverse Dzyaloshinskii-Moriya mechanism for the induced ferroelectricity as proposed in Ref. 24. However, as we will show below, the cycloid structure is strongly distorted via spin-lattice coupling.

Figure 2 shows representative L -scans along both (0 0 L) and (2 0 L) directions. The scattering intensity is plotted on a logarithmic scale. Fig. 2 (a) compares the L -scans along (0 0 L) measured at 1.5 K and 10 K. Besides the strong, primary IC satellite peaks, additional weak reflections are clearly observed at 1.5 K that can be indexed as 2nd, 3rd and 5th-order harmonics of the wave vector k_1 . Furthermore, weak commensurate peaks with a propagation vector $k_2=(0\ 0\ k_{z2})$ ($k_{z2}=0.25$) are also observed at 1.5 K. As depicted in Fig. 2 (b), both (2 0 0.23) IC and (2 0 0.25) commensurate peaks are observed in the L -scan along (2 0 L). The inset illustrates the temperature dependence of (2 0 0.23) and (2 0 0.25). Both reflections show increased intensity with decreasing temperature suggesting they are magnetic in origin. The observed spin texture (both even and odd-order harmonics associated with k_1 and coexistence of the k_2 commensurate phase) indicates the cycloidal spiral spin structure is strongly distorted since no higher-order harmonics should be observed for a perfect cycloid spiral. Furthermore, as discussed in Ref. 26, odd-order harmonics and even order harmonics are expected to be magnetic and nuclear in origin, respectively. The observation of the 2nd-order harmonic provides direct evidence of a lattice modulation associated with the cycloid order with wave vector k_1 .

The magnetic transitions occur within a narrow temperature range at $T_N\approx 7.3$ K and $T_{FE}\approx 6.8$ K. To clarify the nature and exact transition temperature of the primary satellite and higher-order harmonic peaks, we measure both (0 0 0.77)=(0 0 $1-k_{z1}$) and (0 0 2.46)=(0 0 $2+2k_{z1}$) (2nd-order harmonic) as a function of temperature by performing L scans. The obtained order parameters and peak center (indexed using k_{z1}) versus T are plotted in Fig. 3 in comparison with the specific heat data (Fig. 3 (a)). The order parameter of (0 0 0.77) (Fig. 3 (b)) shows a transition at 7.3 K corresponding to T_N and depicts no clear anomaly at T_{FE} . The order parameter of (0 0 2.46) (Fig. 3 (c)) reveals that the appearance of the 2nd-order harmonic coincides with the onset of electric polarization. Fitting the order parameters over the temperature ranges $2\text{ K} < T < T_N$ and $2\text{ K} < T < T_{FE}$ to a power-law $I(T)=I_0[(T_N-T)/T_N]^{2\beta}$ yield $T_N\approx 7.34\pm 0.02$ K and $\beta\approx 0.194\pm 0.015$ for (0 0 0.77), and $T_{FE}\approx 6.68\pm 0.03$ K and $\beta\approx 0.245\pm 0.002$ for (0 0 2.46), respectively. These critical exponent β

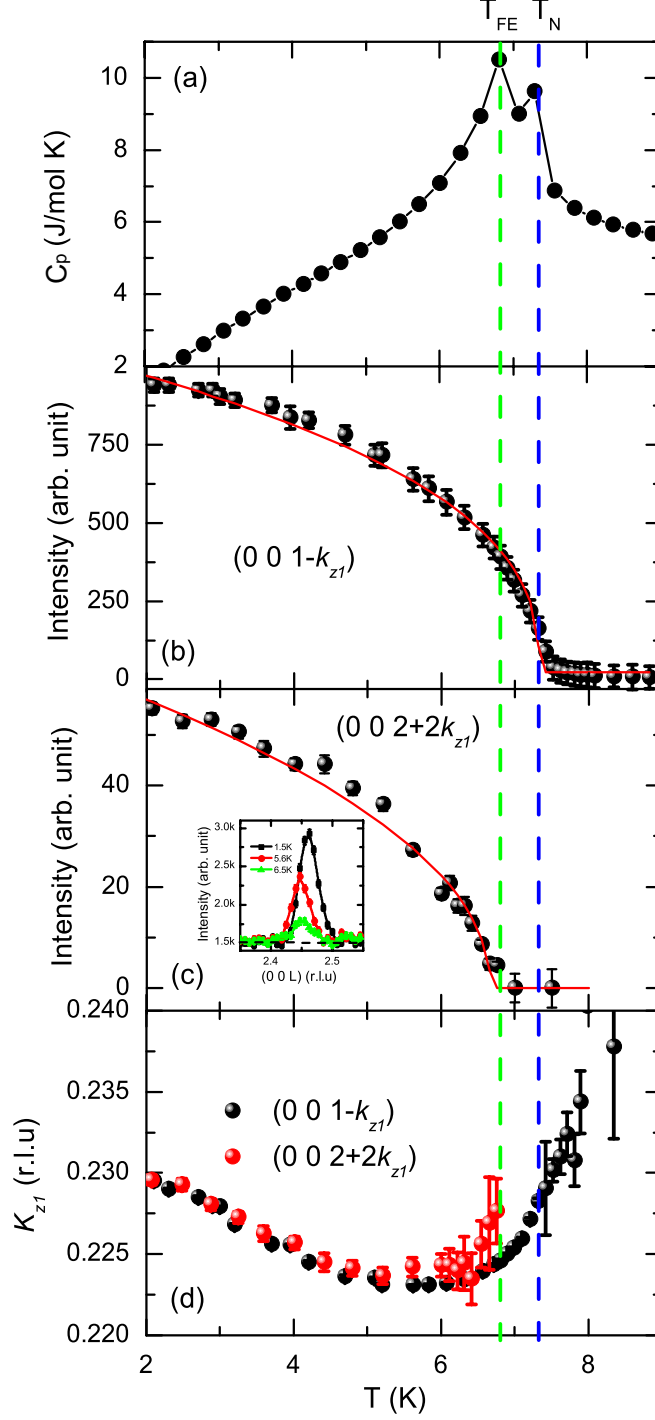


FIG. 3. (Color online) Temperature dependence of (a) the specific heat, (b) integrated intensity of the $(0\ 0\ 0.77)$ magnetic peak, and (c) integrated intensity of the $(0\ 0\ 2.46)$ 2nd-order harmonic peak. The inset in (c) shows L scans of $(0\ 0\ 2.46)$ at selected temperatures. The solid lines in (b) and (c) are fits of the order-parameter data to the power law as described in the text. (d) Temperature dependence of IC propagation vector k_{z1} determined from $(0\ 0\ 1-k_{z1})$, and $(0\ 0\ 2+2k_{z1})$. The error bar in (d) represents statistical error from the fitting, not the systematic error.

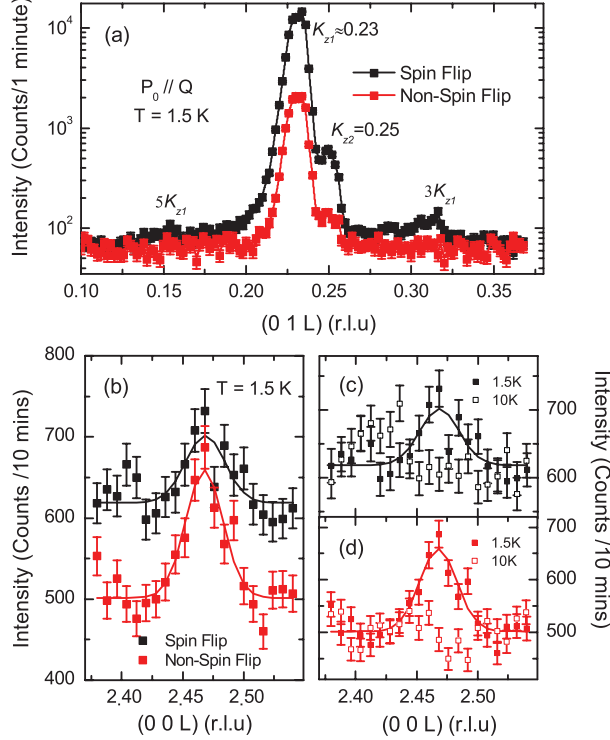


FIG. 4. (Color online) Polarized neutron data measured in the horizontal field configuration, $P_0 \parallel Q$. (a) L-scan along $[0\ 1\ L]$ measured at 1.5 K comparing the spin-flip (SF, $-+$) and non-spin-flip (NSF, $++$) scatterings with the intensity plotted on a logarithmic scale. (b) Comparison of the 1.5 K SF and NSF data suggests the hybrid nature of the $(0\ 0\ 2.46)$ 2nd-order harmonic peak. Comparison of 1.5 K and 10 K data of $(0\ 0\ 2.46)$ from (c) SF channel and (d) NSF channel, respectively.

values are much smaller than the theoretical value of 0.36 predicted for a three-dimensional Heisenberg antiferromagnet (de Jongh and Miedema 1974). This suggests a lower magnetic dimensionality of $(\text{ND}_4)_2\text{FeCl}_5 \cdot \text{D}_2\text{O}$ as proposed in Ref. 21. The temperature dependence of the IC propagation vector k_{z1} , determined by fitting the L -scans of $(0\ 0\ 0.77)$ and $(0\ 0\ 2.46)$, is plotted in Fig. 3 (d). Good agreement is obtained between $2\ \text{K} < T < 6\ \text{K}$, the discrepancy above 6 K can be attributed to the significant broadening of both reflections near T_{FE} and T_N . The wave vector $(0\ 0\ k_{z1})$ continues to vary with decreasing temperature throughout the ferroelectric phase and it shows no evidence of an incommensurate-commensurate (IC-C) lock-in transition down to 1.5 K.

A polarized neutron diffraction experiment was carried out to clarify the origin of the higher-order harmonics and k_2 -type commensurate peaks. Fig. 4 plots the polarized data analyzed using the method discussed in Ref. 27. The magnetic origin of the commensurate peak and the odd-order harmonics associated with the cycloid order is verified by the stronger

scattering observed in the spin-flip (SF, $-+$) channel in Fig. 4 (a). The remaining scattering in the non-spin-flip (NSF, $++$) channel can be attributed to finite instrumental flipping ratio which is estimated to be $\sim 1/10$ by comparing the integrated intensity of SF and NSF data of the (0 0 2) nuclear peak. Fig. 4 (b) compares the SF and NSF data of (0 0 2.46) measured at 1.5 K. Stronger scattering intensity is detected in the NSF channel indicating the 2nd-order harmonic is dominated by nuclear scattering contribution. Weak scattering is also observed in the SF channel. The integrated intensity ratio between NSF and SF is ~ 1.8 , much smaller than the ratio of ~ 10 obtained for the nearby (0 0 2) nuclear peak, suggesting a hybrid nature displaying both nuclear and magnetic characters. Fig. 4 (c) and (d) compares 1.5 K and 10 K data measured with SF and NSF configurations, respectively. In both cases, the (0 0 2.46) peak vanishes at 10 K in good agreement with the order parameter results measured with unpolarized neutrons.

We find the spin texture (in the form of higher-order harmonics) observed in $(\text{ND}_4)_2\text{FeCl}_5 \cdot \text{D}_2\text{O}$ is strikingly similar to that of TbMnO_3 , a well studied type-II multiferroic system [3–9]. Three transitions are observed in TbMnO_3 at 41 K, 27 K, and 7 K [3], in which the transition at 27 K is accompanied by a dielectric anomaly and electric polarization, whereas the transitions at 41 K and 7 K are associated with the magnetic LRO order of Mn^{3+} and Tb^{3+} , respectively. It has been clarified by a neutron diffraction study [8] that this 27 K transition is associated with a magnetic structure change from an IC sinusoidally modulated collinear magnetic structure to an IC noncollinear spiral. Strong odd-order harmonics are observed indicating the spiral spin configuration is strongly distorted. In particular, the observation of a 2nd-order harmonic associated with chiral wave vector [3] ignited a debate of the FE mechanism between the “pure electronic” model by Katsura, Nagaosa, and Balatsky [28] that suggests the electric polarization can be induced without the involvement of lattice degrees of freedom, and the “ion displacement” model that suggests a lattice distortion via spin-orbit coupling is essential for the FE polarization [4–7]. A resonant x -ray diffraction study [9] reveals the melting of the chiral order associated with the onset of the electric polarization at 27 K, in which the 2nd-order harmonic is unambiguously detected with an order parameter behaving similarly to what we observed in $(\text{ND}_4)_2\text{FeCl}_5 \cdot \text{D}_2\text{O}$. The intensity of the 2nd-order harmonic increases sharply at 27 K coinciding with the onset of the ferroelectricity. These experimental results combined with theory [4–7] have classified TbMnO_3 as a prototypical material in which a cycloidal-spin structure generates an electric

polarization via the spin-orbit interaction.

Comparing our results to TbMnO_3 , it is quite remarkable that almost identical behavior (spin texture) is observed in a molecular compound like $(\text{ND}_4)_2\text{FeCl}_5\cdot\text{D}_2\text{O}$. Both even and odd-order harmonics are observed. Similarly, the magnetic structure of $(\text{ND}_4)_2\text{FeCl}_5\cdot\text{D}_2\text{O}$ changes from IC collinear sinusoidal to IC cycloidal-spiral at T_{FE} without an IC-C lock-in transition. The material is paraelectric between $T_{FE} < T < T_N$ and ferroelectricity only sets in below T_{FE} , where the 2nd-order harmonic appears. Our neutron results provide direct evidence that the onset of the electric polarization is accompanied by a lattice modulation. Combined with the large magnetostriction and negative thermal expansion [19] which are characteristics of strong spin-lattice coupling, our diffraction work indicate the spin-lattice plays a critical role in the FE mechanism in $(\text{NH}_4)_2\text{FeCl}_5\cdot\text{H}_2\text{O}$. Moreover, the observed coexistence of incommensurate and commensurate phases adds additional complexity in this material compared with TbMnO_3 . A preliminary inelastic neutron scattering study suggests incommensurate and commensurate phases are both energetically favorable and the competition between these two phases is responsible for the rich magnetic field versus temperature phase diagram of $(\text{ND}_4)_2\text{FeCl}_5\cdot\text{D}_2\text{O}$ [29].

Two interesting features are present in this molecular compounds. First, although the Fe^{3+} ions in $(\text{NH}_4)_2\text{FeCl}_5\cdot\text{H}_2\text{O}$ are in the high spin state with half-filled $3d^5$ configuration, the measured Fe^{3+} magnetic moment is $\sim 4 \mu_B$ instead of $5 \mu_B$. A large reduction in the saturated spin moment ($\sim 20\%$) reveals the involvement of metal-ligands delocalization as confirmed in previous polarized neutron study [30]. Such hybridization has been reported to play a central role in several Fe^{3+} magnetoelectric oxides via different mechanisms, such as anisotropic Fe-O bonding induced by the lattice distortions with Fe^{3+} ion shifts in GaFeO_3 [31] and d-p hybridization mechanism in $\text{CuFe}_{1-x}\text{Al}_x\text{O}_2$ [32]. Consequently, we hypothesize the metal-ligands hybridization may also play an important role in the FE mechanism in $(\text{NH}_4)_2\text{FeCl}_5\cdot\text{H}_2\text{O}$. Secondly, the fact that $(\text{NH}_4)_2\text{FeCl}_5\cdot\text{H}_2\text{O}$ is the only compound that exhibits magnetically induced electric polarization in the $A_2[\text{FeX}_5\cdot\text{H}_2\text{O}]$ series underscores the critical role of the NH_4 group. Although many ionic salts containing NH_4 are ferroelectric materials [33] and the incorporation of NH_4 has been used as a strategy to search for new multiferroics, only type-I multiferroics (in which the ferroelectricity is typically induced via the disorder-order transition of the NH_4 group at high temperature, and is decoupled to the low temperature magnetic order) have been discovered through this approach so far [16–

18]. It is interesting that $(\text{NH}_4)_2\text{FeCl}_5\cdot\text{H}_2\text{O}$ remains paraelectric below the disorder-order transition at 79 K and the ferroelectricity only sets in at a much lower temperature T_{FE} . One possible scenario is that the replacement of NH_4 for alkali metals further enhances the magnetic frustration to an already frustrated magnetic lattice [23] and the relief of magnetic frustration via a strong spin-lattice coupling generates the ferroelectricity.

In summary, our neutron diffraction study on $(\text{ND}_4)_2\text{FeCl}_5\cdot\text{D}_2\text{O}$ reveals that the appearance of ferroelectricity in this molecular magnet is mediated by spin-lattice coupling. The observed subtle distorted spin texture is remarkably similar to TbMnO_3 which have been clarified to play a critical role in the FE mechanism for this prototypical system. Our results suggest $(\text{ND}_4)_2\text{FeCl}_5\cdot\text{D}_2\text{O}$ is a rare molecular analogue to TbMnO_3 , yet it has a more complex B versus T phase diagram [19, 29]. We believe the exotic magnetic properties are closely related to the effects of Fe-Cl metal-ligands delocalization and the disorder-order transition associated with the NH_4 group. $(\text{ND}_4)_2\text{FeCl}_5\cdot\text{D}_2\text{O}$ can serve as a test bed for molecular cycloidal multiferroicity given that the rich physics displayed in this system can be measured experimentally and directly compared to theory to test theoretical models. The spin-lattice coupling mediated FE mechanism revealed in this system certainly opens an avenue for investigating new molecular and MOFs multiferroics and calls for more thorough theoretical investigations.

ACKNOWLEDGEMENT

The research work at ORNLs High Flux Isotope Reactor and Spallation Neutron Source was sponsored by the Scientific User Facilities Division, Office of Basic Energy Sciences, US Department of Energy. JQY, BCS and RSF were supported by the Department of Energy, Office of Science, Basic Energy Sciences, Materials Sciences and Engineering Division.

Note: While working on the revision of this paper, we become aware of a recent work by Rodríguez-Velamazán et al. which reports that no higher-order harmonics and coexistence of the IC and C phases were observed in their experiment on the same material [34]. We attribute this discrepancy to the better sensitivity to weak reflections in our experiment as explained in the supplemental material [25].

* wt6@ornl.gov

- [1] Sang-wook Cheong and Maxim Mostovoy, Nat. Mater (London), **6**, 13-20 (2007).
- [2] Daniel Khomskii, Physics **2**, 20 (2009).
- [3] T. Kimura, T. Goto, H. Shintani, K. Ishizaka, T. Arima, and Y. Tokura, Nature (London) **426**, 55 (2003).
- [4] I. A. Sergienko and E. Dagotto, Phys. Rev. B **73**, 094434 (2006).
- [5] H. J. Xiang, S.-H. Wei, M.-H. Whangbo, and J. L. F. Da Silva, Phys. Rev. Lett. **101**, 037209 (2008).
- [6] Andrei Malashevich and David Vanderbilt, Phys. Rev. Lett. **101**, 037210 (2008).
- [7] I. V. Solovyev, Phys. Rev. B **83**, 054404 (2011).
- [8] M. Kenzelmann, A. B. Harris, S. Jonas, C. Broholm, J. Schefer, S. B. Kim, C. L. Zhang, S.-W. Cheong, O. P. Vajk, and J.W. Lynn, Phys. Rev. Lett. **95**, 087206 (2005).
- [9] S. W. Lovesey, V. Scagnoli, M. Garganourakis, S. M. Koohpayeh, C Detlefs and U Staub, J. Phys.: Condens. Matter **25**, 362202 (2013).
- [10] K. Taniguchi *et al.*, Phys. Rev. Lett. **97**, 097203 (2006).
- [11] G. Lawes *et al.*, Phys. Rev. Lett. **95**, 087205 (2005).
- [12] R. Vilarreal, G. Quirion, M. L. Plumer, M. Poirier, T. Usui, and T. Kimura, Phys. Rev. Lett. **109**, 167206 (2012).
- [13] H. J. Xiang and M.-H. Whangbo, Phys. Rev. Lett. **99**, 257203 (2007).
- [14] Y. J. Choi, H. T. Yi, S. Lee, Q. Huang, K. Kiryukhin, and S.-W. Cheongs. Phys. Rev. Lett. **100**, 047601 (2008).
- [15] Omar M. Yaghi et al. Nature 423, 705 (2003).
- [16] Raghavendra Samantaray, Ronald J. Clark, Eun S. Choi, and Naresh S. Dalal, J. Am. Chem. Soc. **134**, 15953-15962 (2012).
- [17] Guan-Cheng Xu et al. J. Am. Chem. Soc. **133**, 14948-14951 (2011).
- [18] R. Samantaray et al. J. Am. Chem. Soc., **133**, 3792-3795 (2011).
- [19] M Ackermann, D Brüning, T Lorenz, P Becker, and L Bohatý, New Journal of Physics **15**, 123001 (2013).
- [20] Carlin R L *et al.*, J. Am. Chem. Soc. **99** 7728 (1977).

- [21] J. N. McElearney, and S. Merchant, *Inorganic Chemistry*, Vol. **17**, No. 5,(1978).
- [22] M Gabás, F Palacio, J Rodriguez-Carvajal, and D Visser, *J. Phys.: Condens. Matter* **7**, 4725-4738 (1995).
- [23] Javier Campo, Javier Luzón, Fernando Palacio, Garry J. McIntyre, Angel Millán, and Andrew R. Wildes, *Phys. Rev. B* **78**, 054415 (2008).
- [24] Jose Alberto Rodriguez-Velamazán, Oscar Fabelo, Angel Millan, Javier Campo, Roger D. Johnson, and Laurent Chapon, *Scientific Reports*, 5:14475, DOI: 10.1038/srep14475.
- [25] For crystal growth and experimental details, see supplementary information.
- [26] K. Hirai, *J. Phys. Soc. Jpn.* **66**, 560 (1997).
- [27] R. M. Moon, T. Kiste, and W. C. Koehler, *Phys. Rev.* **181**, 920 (1969).
- [28] H. Katsura, N. Nagaosa, and A. V. Balatsky, *Phys. Rev. Lett.* **95**, 057205 (2005).
- [29] W. Tian et al. unpublished.
- [30] Javier Luzón, Javier Campo, Fernando Palacio, Garry J. McIntyre, and Angel Millán, *Phys. Rev. B* **78**, 054414 (2008).
- [31] J.-Y. Kim, T.Y. Koo, and J.-H. Park, *Phys. Rev. Lett.* **96**, 047205 (2006)
- [32] Taro Nakajima, Setsuo Mitsuda, Toshiya Inami, Noriki Terada, Hiroyuki Ohsumi, Karel Prokes and Andrei Podlesnyak, *Phys. Rev. B* **78**, 024106 (2008).
- [33] A. H. Rama Rao, M. R. Srinivasan, H. L. Bhat and P. S. Narayana, *Ferroelectrics* **21** 433(1978).
- [34] J. Alberto Rodriguez-Velamazán, Oscar Fabelo, Javier Campo, Angel Millan, Juan Rodriguez-Carvajal, and Laurent C. Chapon, arXiv:1608.02369.